



# A Novel Optical Intracellular Imaging Approach for Potassium Dynamics in Astrocytes

Theresa S. Rimmele<sup>1</sup>, Jean-Yves Chatton<sup>1,2\*</sup>

**1** Department of Fundamental Neurosciences, University of Lausanne, Lausanne, Switzerland, **2** Cellular Imaging Facility, University of Lausanne, Lausanne, Switzerland

## Abstract

Astrocytes fulfill a central role in regulating  $K^+$  and glutamate, both released by neurons into the extracellular space during activity. Glial glutamate uptake is a secondary active process that involves the influx of three  $Na^+$  ions and one proton and the efflux of one  $K^+$  ion. Thus, intracellular  $K^+$  concentration ( $[K^+]_i$ ) is potentially influenced both by extracellular  $K^+$  concentration ( $[K^+]_o$ ) fluctuations and glutamate transport in astrocytes. We evaluated the impact of these  $K^+$  ion movements on  $[K^+]_i$  in primary mouse astrocytes by microspectrofluorimetry. We established a new noninvasive and reliable approach to monitor and quantify  $[K^+]_i$  using the recently developed  $K^+$  sensitive fluorescent indicator Asante Potassium Green-1 (APG-1). An *in situ* calibration procedure enabled us to estimate the resting  $[K^+]_i$  at  $133 \pm 1$  mM. We first investigated the dependency of  $[K^+]_i$  levels on  $[K^+]_o$ . We found that  $[K^+]_i$  followed  $[K^+]_o$  changes nearly proportionally in the range 3–10 mM, which is consistent with previously reported microelectrode measurements of intracellular  $K^+$  concentration changes in astrocytes. We then found that glutamate superfusion caused a reversible drop of  $[K^+]_i$  that depended on the glutamate concentration with an apparent  $EC_{50}$  of  $11.1 \pm 1.4$   $\mu$ M, corresponding to the affinity of astrocyte glutamate transporters. The amplitude of the  $[K^+]_i$  drop was found to be  $2.3 \pm 0.1$  mM for 200  $\mu$ M glutamate applications. Overall, this study shows that the fluorescent  $K^+$  indicator APG-1 is a powerful new tool for addressing important questions regarding fine  $[K^+]_i$  regulation with excellent spatial resolution.

**Citation:** Rimmele TS, Chatton J-Y (2014) A Novel Optical Intracellular Imaging Approach for Potassium Dynamics in Astrocytes. PLoS ONE 9(10): e109243. doi:10.1371/journal.pone.0109243

**Editor:** Alexander A. Mongin, Albany Medical College, United States of America

**Received:** August 4, 2014; **Accepted:** September 9, 2014; **Published:** October 2, 2014

**Copyright:** © 2014 Rimmele, Chatton. This is an open-access article distributed under the terms of the Creative Commons Attribution License, which permits unrestricted use, distribution, and reproduction in any medium, provided the original author and source are credited.

**Data Availability:** The authors confirm that all data underlying the findings are fully available without restriction. All relevant data are within the paper and its Supporting Information file.

**Funding:** This work is supported by grant #31003A-135720 from the Swiss National Science Foundation to JY Chatton. The funders had no role in study design, data collection and analysis, decision to publish, or preparation of the manuscript.

**Competing Interests:** The authors have declared that no competing interests exist.

\* Email: jean-yves.chatton@unil.ch

## Introduction

The gradient of potassium ions across the membrane of mammalian cells, along with that of  $Na^+$ , plays a vital role both in establishing the standing electrical potential and in powering numerous transport systems. In astrocytes, these gradients are critical not only for the maintenance of a cell's own internal homeostasis—such as the regulation of internal pH and ion composition—but they also enable the dynamic regulation of the brain interstitial milieu. Of particular importance, astrocytes play a predominant role in the clearance of neurotransmitters released in the synaptic cleft by neurons during synaptic activity [1]. They are also actively involved in taking up extracellular  $K^+$  ( $[K^+]_o$ ) released by neurons during activity, particularly during the action potential repolarization phase [2]. Without adequate regulation, the increase in  $[K^+]_o$  following action potentials would interfere with normal electrical activity and rapidly abolish network activity [2,3]. Astrocytes express both active and passive mechanisms for  $K^+$  uptake and release, such as the inwardly rectifying potassium channel 4.1 ( $K_{ir}$  4.1) [2,4], the  $Na^+/K^+/Cl^-$  cotransporter, and the  $Na^+/K^+$  ATPase [5,6], and together these provide a highly efficient mechanism for rapid regulation of  $K^+$  by astrocytes in the brain. As a consequence of being extensively interconnected by gap junctions, astrocytes are capable of redistributing  $K^+$  to distant sites through the astrocytic syncytium [2].

Intracellular  $Na^+$  has been shown to undergo sizeable changes during activity [7]. This  $Na^+$  influx is caused in particular by the  $Na^+$ -dependent uptake of glutamate, which has been identified to play a key role in the neuron-glia metabolic communication [8]. Glial glutamate uptake accomplished through as a secondary active process that involves the influx of three  $Na^+$  ions and one proton and the efflux of one  $K^+$  ion [9–11]. Therefore, intracellular  $K^+$  can be expected to undergo variations due to glutamate transport activity.

Thus,  $[K^+]_i$  is potentially influenced both by  $[K^+]_o$  fluctuations and by glutamate transport activity in astrocytes. It has been shown that  $K^+$  accumulates in astrocytes in response to increases in  $[K^+]_o$  in slices and in cultured astrocytes of several species [12–16]. However, little is known regarding whether and how the intracellular  $K^+$  concentration is influenced by the transmembrane ion fluxes associated with glutamate uptake in astrocytes.

Ion-selective electrodes have been extensively used for extracellular  $K^+$  measurements (see e.g. [17,18]). They have also been used for intracellular measurements of  $K^+$  concentration in the studies referenced above [12–16]. However, these approaches are relatively invasive and do not provide direct spatial information about  $K^+$  changes. Fluorescence-based detection of  $[K^+]_i$  offers the benefits of being both non-invasive and capable of assessing the spatiotemporal pattern of  $K^+$  flux within the tissue. This approach,

however, has not been straightforward to implement. The only available fluorescent dye to date, the ultraviolet probe Potassium-binding benzofuran isophthalate (PBFI) is difficult to load intracellularly, displays weak fluorescence, and has a  $K_d$  for  $K^+$  of  $\sim 8$  mM [19] that is far from the expected  $[K^+]_i$  range, which is normally  $>100$  mM. For these reasons, only a few reports have demonstrated successful use of this probe (see e.g. [17,20,21]).

The aims of the present study were (1) to characterize a novel  $K^+$ -sensitive indicator named Asante Potassium Green-1 (www.teflabs.com) for its potential use as noninvasive and reliable tool to monitor and quantify  $[K^+]_i$  during glial activity; (2) to employ this tool to investigate how  $[K^+]_i$  changes in response to  $[K^+]_o$  fluctuations and to glutamate application in primary mouse astrocytes. This new fluorescent indicator enabled us to demonstrate that primary mouse astrocytes display significant  $[K^+]_i$  changes in the order of several millimolar both in response to  $[K^+]_o$  level changes and to glutamate transporter activation. These changes likely play an important role in the integrated functions of astrocytes that are involved both in  $[K^+]_o$  and extracellular glutamate regulation.

## Materials and Methods

### Cell culture

Every effort was made to minimize suffering and the number of animals used in all experiments. All experimental procedures were carried out in strict accordance with the recommendations of the Swiss Ordinance on Animal Experimentation and were specifically approved for this study by the Veterinary Affairs Office of the Canton of Vaud, Switzerland (authorization number 1288.5). Primary cultures of cortical astrocytes were prepared from 1 to 3-days-old C57Bl6 mice as described elsewhere [22]. Astrocytes were cultured for 3–4 weeks in DME medium (Sigma) supplemented with 10% FCS before experiments and were plated on glass coverslips for imaging.

### Spectrofluorimetry

The free acid form of the dye Asante Potassium Green-1 (APG-1) TMA salt or APG-2 TMA salt were used for the *in vitro* characterization. Fluorimetric analysis was performed in quartz cuvettes using a Perkin Elmer model LS55 luminescence/fluorescence spectrometer. Intracellular-like solutions were used for titrations and contained (mM): 12 NaCl, 5  $MgCl_2$ , 0.5  $CaCl_2$ , 1 EGTA, 10 HEPES, adjusted to pH 7.2 using N-methyl-D-glucuronate. The  $K^+$  titration of the dye was obtained by successive additions of known amounts of  $K^+$ -gluconate. The  $K^+$  selectivity of APG-1 over  $Na^+$  was analyzed using solutions containing (mM): 135  $K^+$  gluconate, 5  $MgCl_2$ , 0.5  $CaCl_2$ , 1 EGTA, 10 HEPES, adjusted to pH 7.2 using N-methyl-D-glucamine, and increasing amounts of NaCl were added. For each  $K^+$  or  $Na^+$  concentration, emission spectra were recorded. Intracellular excitation spectra were recorded in living cells using a monochromator coupled to a Xenon arc lamp (Polychrome II, Till Photonics, Planegg, Germany) attached to an inverted fluorescence microscope (see below). Emission spectra following excitation at 488 nm were obtained using a LSM710 confocal microscope equipped with spectral detector (Carl Zeiss).

### Fluorescence microscopy

Dye-loaded cells were placed in a thermostated chamber designed for the rapid exchange of perfusion solutions and observation using oil-immersion objectives [23]. Cells were superfused at 35°C. Low-light level fluorescence imaging was performed on an inverted epifluorescence microscope (Axiovert

100 M, Carl Zeiss) using a 40 $\times$ 1.3 N.A. oil-immersion objective lens. Fluorescence excitation wavelengths were selected using a monochromator (Till Photonics) and fluorescence was detected using a 12-bit cooled CCD camera (Princeton Instruments) or EM-CCD camera (Andor). Image acquisition was computer-controlled using the software Metafluor (Universal Imaging, Reading, PA). Images were acquired at 0.2 to 1 Hz.

Experimental solutions contained (mM) NaCl, 137.4; KCl, 5.4;  $NaHCO_3$ , 25;  $CaCl_2$ , 1.3;  $MgSO_4$ , 0.8; and  $NaH_2PO_4$ , 0.78; glucose, 5, bubbled with 5%  $CO_2$ /95% air. When using different  $K^+$  concentrations, NaCl was adjusted to maintain isotonicity. Solutions for dye loading contained (mM) NaCl, 160; KCl, 5.4; HEPES, 20;  $CaCl_2$ , 1.3;  $MgSO_4$ , 0.8;  $NaH_2PO_4$ , 0.78; glucose, 20 and were supplemented with 0.1% Pluronic F-127 (Molecular Probes, Eugene, OR). In experiments involving more than one solution application, the order was alternated in order to exclude order-related effects. In this study, the standard reference  $[K^+]_o$  of 5.4 mM was chosen to enable direct comparison with previous studies from our and other laboratories in the field of astrocyte research [23–25].

$[K^+]_i$  was monitored by loading astrocytes at 37°C for 40 min with the acetoxymethyl ester membrane permeant form of the dye APG-1 AM (12  $\mu$ M) as described in [26]. APG-1 fluorescence was excited at 515 nm and detected at 535–585 nm (Chroma, Rockingham, VT). A similar *in situ* calibration procedure as previously described in mesangial cells and cerebellar granule cells was used as previously described [20,27]. Briefly, astrocytes were permeabilized using 10  $\mu$ g/ml nigericin and 10  $\mu$ M valinomycin with simultaneous inhibition the  $Na^+/K^+$ -ATPase using 1 mM ouabain. Cells were then sequentially perfused with solutions buffered at pH 7.2 with 20 mM HEPES and containing 160, 140, 120 and 100 mM  $K^+$ , respectively, and 30 mM  $Cl^-$ , 135 mM gluconate with a constant total concentration of  $Li^+$  and  $K^+$  of 160 mM, replacing  $K^+$  by  $Li^+$  in the solution and keeping constant  $Na^+$  and  $Cl^-$  concentrations. The *in situ* calibration procedure was performed for each cell at the end of experiments where the  $K^+$  concentration is displayed in the graph ordinate, as described in previous studies on intracellular  $Na^+$  or pH (see e.g. [23,28]).

Experiments using Sodium-binding benzofuran isophthalate (SBFI-AM, 15  $\mu$ M, excited at 340 nm and 380 nm) or Fura-2 AM (8  $\mu$ M, excited at 360 nm) together with APG-1 AM (excited at 490 nm) were performed using similar protocol as previously described [29]. For these experiments, the emitted fluorescence was detected through a 535 nm (35-nm bandpass) interference filter (Omega Optical, Brattleboro, VT).

For experiments requiring local delivery of  $K^+$ , dye-loaded cells were placed in a customized open chamber enabling rapid exchange of perfusion solutions. A glass pipette of tip diameter 1–2  $\mu$ m was filled with 500 mM  $K^+$ -gluconate, approached using a micromanipulator (Sutter Instruments) at a distance of  $\sim 10$   $\mu$ m from the cells. Pressure pulses of 200–500 ms, 1–2 psi were applied to the back of the pipette using a Picospritzer III (Sensortech, Puchheim, Germany) to locally deliver  $K^+$ .

### Data analysis and statistics

Fluorescence intensity traces were drawn from regions of interest selected in up to 10 individual cells from the field of view using the Metafluor software package. Further calculations were done with Excel (Microsoft). Graphs and curve fitting were done with Kaleidagraph (Synergy Software, Reading, PA, USA). Unless otherwise indicated, a paired Student's *t* test was performed for each experimental group to assess the statistical significance against respective controls, \*, \*\*, and \*\*\* refer to *p* values of 0.05, 0.01, and 0.001, respectively. For estimation of  $EC_{50}$  values, non-linear curve

fitting was performed using the Levenberg-Marquardt algorithm implemented in the Kaleidagraph software package. The equation used for fitting the dose-response analysis experiments is the following:

$$F_{obs} = F_{max} \cdot [A] / (K + [A]) + F_{min} \quad (1)$$

were  $F_{obs}$  is the observed response,  $F_{max}$ ,  $F_{min}$  are maximum, minimum parameters of the response.  $[A]$  is the concentration of agonist and  $K$  is the agonist concentrations that yield half-maximum responses (*i.e.* EC<sub>50</sub>). Equation [1] corresponds to a one-site Michaelis-Menten model.

## Dyes and drugs

Nigericin was from Abcam (Cambridge, UK), valinomycin from Fluka (Buchs, Switzerland). All other chemicals were from Sigma-Aldrich (Buchs, Switzerland).

## Results

### APG-1 characterization

In a first phase, the K<sup>+</sup> sensitivity and selectivity of the APG-1 fluorescent indicator was characterized *in vitro* using spectrofluorimetry. APG-1 is based on a similar design as the very successful sodium version Asante Natrium Green-1 [26]. For this purpose, APG-1 was dissolved in solutions corresponding to intracellular ionic composition, *i.e.* containing 10 mM Na<sup>+</sup>, nanomolar Ca<sup>2+</sup> and millimolar Mg<sup>2+</sup> concentration at pH 7.2. Excitation spectra presented a peak at ~515 nm (*not shown*), whereas emission spectra had a maximum at ~540 nm (**Fig. 1A**), thus exhibiting spectral properties very similar to the related Na<sup>+</sup> indicator Asante Natrium Green-1 [26]. Changing K<sup>+</sup> concentration from 0 to 150 mM caused stepwise increases in fluorescence emission. APG-1 fluorescence emission versus K<sup>+</sup> concentration (**Fig. 1B**) displayed a monotonic increase up to the expected upper physiological K<sup>+</sup> concentration range of 150 mM. Neither the excitation nor the emission spectra displayed a shift in their maxima with increasing K<sup>+</sup> concentration. The K<sup>+</sup>-sensitivity of the related indicator APG-2 was analyzed in parallel experiments. **Fig. 1B** shows that APG-2, as indicated by the manufacturer, has a higher affinity for K<sup>+</sup> in identical intracellular-like solutions. APG-2 fluorescence reached saturation at K<sup>+</sup> concentrations higher than ~80 mM. This result indicates that APG-2 is unlikely to respond to K<sup>+</sup> changes at physiological intracellular concentrations. Our tests performed with intracellular APG-2 (loaded using its membrane permeant form) confirmed this prediction, as no change or very small fluorescence changes were observable during cell stimulations such as by glutamate applications (*not shown*).

We next tested for potential influence of Na<sup>+</sup>, which is known to undergo rapid and substantial amplitude changes in astrocytes in the range 10–30 mM [7,23,30], in particular during glutamate transporter activity. **Fig. 1C** shows that Na<sup>+</sup> concentrations up to 50 mM had only marginal influence on APG-1 fluorescence. **Fig. S1** extends this analysis and shows the effect of Na<sup>+</sup> on APG-1 for different K<sup>+</sup> concentrations ranging from 0 to 150 mM. It was found that in the absence of K<sup>+</sup> the indicator displayed an expected increased sensitivity to Na<sup>+</sup>. However, for K<sup>+</sup> concentrations within the range of intracellular levels ([K<sup>+</sup>]<sub>i</sub> > 100 mM), the interaction with Na<sup>+</sup> was found to be minimal.

APG-1 is a weak acid, like other related fluorescent indicators of cations, and therefore it is potentially influenced by pH. We therefore tested whether pH had an influence on APG-1 fluorescence. **Fig. 1D** shows that the fluorescence of APG-1 was

stable within the pH range of 7–8, found *in vivo* in brain cells under normal conditions. The figure also shows however that APG-1 fluorescence tends to decline below pH~6.8, which should be taken into account in experiments involving substantial cellular acidification.

In summary, APG-1 is a fluorescent indicator in the visible light spectrum that displays in cuvette properties that make it very promising for intracellular K<sup>+</sup> concentration measurements.

In the next series of experiments, astrocytes were then loaded using the membrane permeant form of the dye, APG-1 AM. Cultured astrocytes adopt an extremely flat morphology (cell thickness typically ~1–2 μm) with the nucleus being the thickest part of the cell (typically 5–8 μm). When loaded with indicators with cytosolic localization that have the ability to permeate through nuclear pores, wide-field images of astrocytes show bright fluorescent nuclei, as they correspond to the cell region with the largest optical path length. As seen in **Fig. 2A**, cellular loading with APG-1 was strong and exhibited a typical of a cytosolic dye distribution. This property of APG-1 AM contrasts with the poor loading efficiency usually reported for the other K<sup>+</sup>-sensitive dye PBFI AM. Excitation and emission spectra of intracellular APG-1 were then recorded and showed maxima at 522 nm and 547 nm, respectively (**Fig. 2B**). Thus, *in situ*, the dye displays a slight red-shift of its spectra compared with in cuvette measurements. The probe exhibited a remarkable intracellular stability, with negligible photobleaching or cell leakage, as observed previously with the related sodium probe ANG-1 [26]. Next, an *in situ* calibration procedure was developed and optimized, applying general principles used for calibration of Na<sup>+</sup> indicators. After permeabilization of the cell membrane using ionophores and blockade of the Na<sup>+</sup>/K<sup>+</sup> ATPase, solutions with of different K<sup>+</sup> concentration were sequentially applied and the resulting fluorescence signal recorded (**Fig. 2C**). Satisfactory permeabilization was evaluated by the rapid establishment of plateau fluorescence values, that were then plotted against the known K<sup>+</sup> concentration (**Fig. 2D**) to enable retrospective calculation of K<sup>+</sup> concentration variations during the experiment. Under our experimental conditions and using this procedure, the resting [K<sup>+</sup>]<sub>i</sub> was found to average 133 ± 1 mM, which is consistent with expected mammalian cell [K<sup>+</sup>]<sub>i</sub> values [20,21,27].

Taken together, one can conclude from this *in vitro* and intracellular characterization that APG-1 can be safely used as a K<sup>+</sup>-sensitive intracellular indicator.

### [K<sup>+</sup>]<sub>o</sub> level influences the cytosolic K<sup>+</sup> in astrocytes

Because astrocytes are major actors in the regulation of interstitial K<sup>+</sup> in the brain [2], we asked to what extent [K<sup>+</sup>]<sub>i</sub> is influenced by [K<sup>+</sup>]<sub>o</sub>. We therefore loaded primary astrocytes with APG-1 AM and applied different solutions containing K<sup>+</sup> in the expected concentration range that these cells may be exposed to in the brain. **Fig. 3A&B** shows that changing [K<sup>+</sup>]<sub>o</sub> reproducibly caused a change in [K<sup>+</sup>]<sub>i</sub> levels that followed [K<sup>+</sup>]<sub>o</sub> changes proportionally in the range 3–10 mM (slope = 1.04 ± 0.06, n = 120 cells, 12 exp). No further increase in [K<sup>+</sup>]<sub>i</sub> was observed for 15 mM [K<sup>+</sup>]<sub>o</sub>. In addition, the lower slope and the kinetics of the changes with an initial transient, is consistent with some degree of cell volume regulation.

To investigate whether the APG-1 can be used measure responses to rapid and spatially limited [K<sup>+</sup>]<sub>o</sub> elevations on [K<sup>+</sup>]<sub>i</sub>, we applied single short extracellular puffs from a K<sup>+</sup>-gluconate-filled pipette (**Fig. 3C**). [K<sup>+</sup>]<sub>i</sub> rose rapidly with an average amplitude of 2.2 ± 0.2 mM (**Fig. 3D**) and recovered to half amplitude within 26.8 ± 2.6 s (**Fig. 3E**) in close proximity to the pipette tip (upper trace), whereas no responses were found at

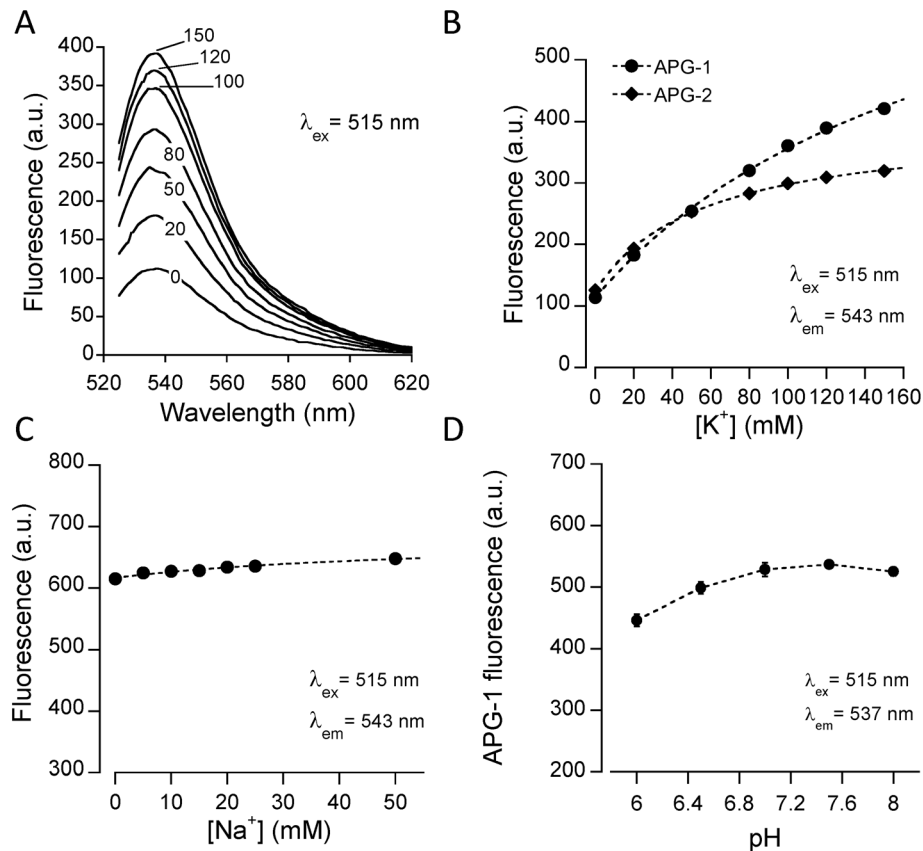


**Figure 1. Spectrofluorimetric characterization of the  $K^+$  indicator APG-1.** (A) Emission spectra recorded in the presence of different  $[K^+]$  in intracellular-like solutions following excitation at 515 nm. Emission maximum was  $\sim 540$  nm. (B) Fluorescence emission plotted as a function of  $[K^+]$  showing a monotonic relationship of APG-1 fluorescence with increasing  $[K^+]$  (circles). The same analysis was performed on APG-2, a related indicator with identical spectral properties (diamonds) but lower  $K_d$  for  $K^+$ . The plots show that APG-2 fluorescence becomes saturated at  $[K^+] > 80$  mM, which is not the case with APG-1. (C)  $Na^+$  dependency of APG-1 fluorescence measured in intracellular-like solution containing 135 mM  $K^+$  (see also Fig. S1). (D) pH dependency of APG-1 fluorescence measured in intracellular-like solution containing 135 mM  $K^+$ . The pH of each solution was adjusted using NMDG. This pH analysis was repeated three times. Data are presented as means  $\pm$  SEM of triplicate measurements.  
doi:10.1371/journal.pone.0109243.g001

distances  $>90$   $\mu M$  (lower trace). Application of 200  $\mu M$   $Ba^{2+}$  did not prevent the initial  $K^+$  influx, but it did decrease the duration of the response (Fig. 3D&E). The mechanism underlying the shortened response duration is currently unclear.

After taking up the transient local excess of  $[K^+]_o$  occurring in the vicinity of activated neurons, astrocytes are thought to redistribute it through the gap junctions over the syncytium towards lower local  $[K^+]_i$ , from whence it eventually returns to the extracellular space [31–33]. We therefore investigated whether gap junctions were involved in shaping the observed  $[K^+]_i$  response. In the presence of carbenoxolone (CBX, 20  $\mu M$ ), a blocker of gap junction [34], the half-time of recovery of  $[K^+]_i$  doubled ( $46.7 \pm 4.3$  s), whereas the amplitude was not significantly altered ( $2.4 \pm 0.3$  mM) (Fig. 3C–E). This result is consistent with the notion of the spatial redistribution of  $K^+$  over the astrocytic syncytium as proposed previously [2,35]. In situations of impaired by gap junction communication,  $K^+$  excess persists longer within single cells.

#### Glutamate transporter activity dynamically influences $[K^+]_i$

Glial high-affinity glutamate transporters have a complex stoichiometry in which glutamate influx is coupled with three  $Na^+$  ions and one proton in exchange with one  $K^+$  ion [10,11].

Activation of this transporter is sufficient to induce substantial  $[Na^+]_i$  changes in astrocytes both in culture and in situ [7,23]. We therefore asked whether the  $K^+$  efflux associated with the glutamate transport cycle could alter  $[K^+]_i$  levels in a detectable manner. Fig. 4A shows a single cell trace during application of glutamate, which caused a reversible decrease in  $[K^+]_i$ . The  $[K^+]_i$  drop induced by 200  $\mu M$  glutamate averaged  $2.3 \pm 0.1$  mM ( $n = 89$  cells, 9 exp) for 200  $\mu M$  glutamate application performed in 5.4 mM external  $K^+$  conditions.

In order to verify whether this  $[K^+]_i$  response was glutamate-concentration dependent, we applied glutamate in the concentration range of 0.1  $\mu M$ –10 mM, and measured the APG-1 fluorescence response. The amplitude of the  $K^+$  response was proportional to the bath concentration of glutamate and followed Michaelis and Menten kinetics (Fig. 4B). Non-linear curve fitting using equation [1] yielded an  $EC_{50}$  of  $11.1 \pm 1.4$   $\mu M$  ( $n = 116$  cells, 12 exp). Thus, both the kinetics exhibited by the  $K^+$  response to glutamate and the apparent affinity of the effect are consistent with a mediation of the effect by glutamate transporters. If this is the case, concurrent  $Na^+$  responses should be seen in cells undergoing a  $K^+$  response. We therefore loaded both the UV  $Na^+$  indicator SBFI and APG-1, which are spectrally compatible. Sequential illumination at 340 nm, 380 nm and 490 nm enabled recording the SBFI fluorescent ratio and the APG-1 fluorescence response,

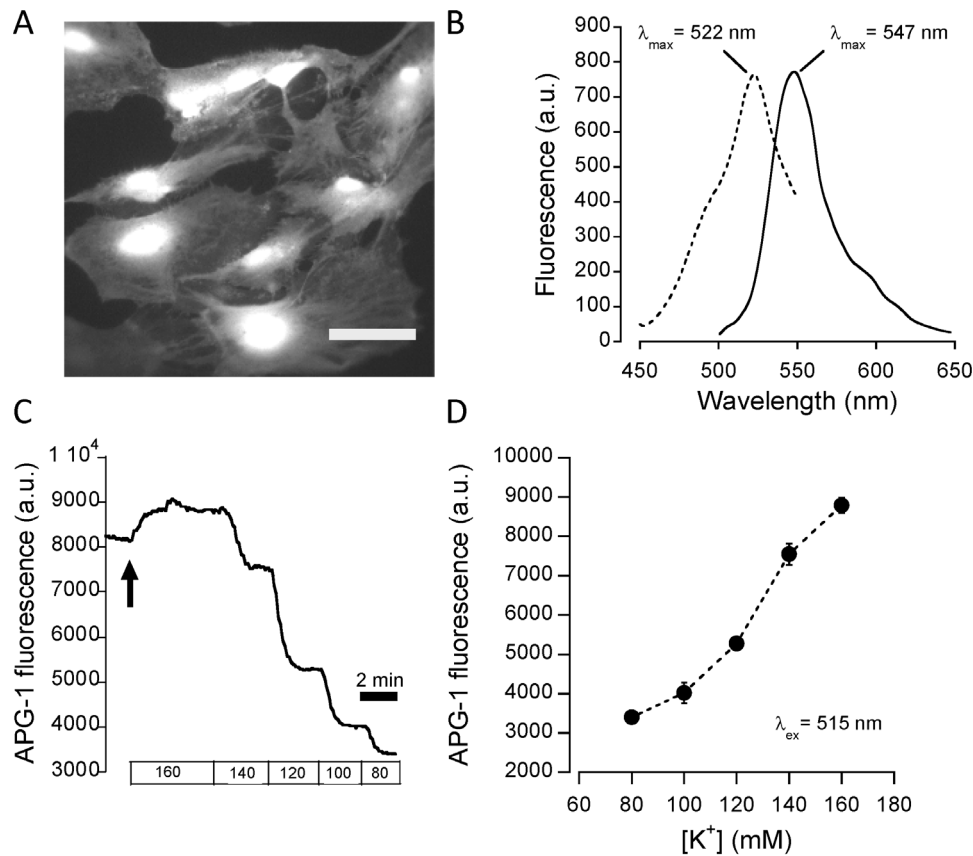


**Figure 2. Intracellular characterization of the  $K^+$  indicator APG-1.** (A) Fluorescence image of primary astrocytes loaded using APG-1 AM. Scale bar 50  $\mu$ m. (B) *In situ* excitation and emission spectra measured by fluorescence microscopy. Intracellular spectra were  $\sim 10$  nm red-shifted compared with measurement in cuvettes. (C) Representative experimental trace depicting the *in situ* calibration procedure. At the time indicated by the arrow, the cell membrane was permeabilized for  $K^+$  using valinomycin and nigericin while the  $Na^+/K^+$  ATPase was inhibited by ouabain. Solutions of different  $[K^+]$  were then sequentially applied until stable fluorescence plateaus were obtained. (D) Calibration curve obtained by plotting the fluorescence plateau values measured for each known  $[K^+]$ .  
doi:10.1371/journal.pone.0109243.g002

reflecting  $Na^+$  and  $K^+$  changes, respectively, in the same cell. **Fig. 4C** shows that astrocytes displayed opposite responses to glutamate, compatible with the activation of glutamate transporters causing both an increase in  $Na^+$  and a decrease in  $K^+$  with similar kinetics. In comparison, we loaded the UV probe Fura-2, and illuminated it at its isosbestic—*i.e.*  $Ca^{2+}$ -insensitive—wavelength. Whereas APG-1 showed a downward fluorescence response to glutamate, Fura-2 at 360 nm yielded no fluorescence change in response to glutamate, indicating the absence of cell swelling that could have participated in the APG-1 fluorescence decrease.

## Discussion

Normal brain activity involves substantial movements of ions secondary to the generation of action potentials. In particular, neuronal excitation leads to elevations of extracellular  $K^+$  levels that have to be rapidly normalized in order to enable subsequent activity [3]. Of equal importance, concurrent excitatory neurotransmitter glutamate released from activated synapses, must be removed from the interstitial space to cope with high frequency synaptic transmission and prevent excitotoxic glutamate accumulation. Astrocytes play a central role in both these processes, which makes them essential players in the regulation of neuronal activity. In the present study, we employed a novel  $K^+$ -sensitive fluorescent

indicator to demonstrate that  $[K^+]_i$  is significantly influenced by both external  $K^+$  and by glutamate transport activity.

Intracellular  $K^+$  measurements have been hampered until now by the lack of adequate fluorescent probe. The only one previously available, PBFI, suffers from a low quantum yield, a poor selectivity for  $K^+$  over  $Na^+$ , an ultraviolet excitation, as well as an affinity for  $K^+$  of  $\sim 8$  mM [19] that renders it poorly sensitive to  $K^+$  in its physiological intracellular range of  $>100$  mM. Moreover, the membrane permeant form of this dye is notoriously difficult to load in mammalian cells. For the present study, we used the recently synthesized  $K^+$  probe APG-1 and characterized its basic properties both in cuvette and *in situ*. We found that APG-1 generates important fluorescence changes in response to  $K^+$  concentration changes, and is not saturated at physiological intracellular  $K^+$  levels, *i.e.* above 100 mM. Contrary to PBFI (see e.g. [27]), APG-1 fluorescence is only marginally influenced by  $Na^+$  and by pH at their respective physiologically relevant intracellular levels. The spectral properties of APG-1 are very similar to those of the related  $Na^+$  indicator ANG-1 recently described [26]. As with this latter indicator, the membrane-permeant form of APG-1 readily loads into astrocytes and yields a bright and evenly distributed fluorescence, indicating a predominant cytosolic localization. Peak excitation and emission measured intracellularly were found to be red shifted by  $\sim 10$  nm compared with measurements performed in cuvettes. This

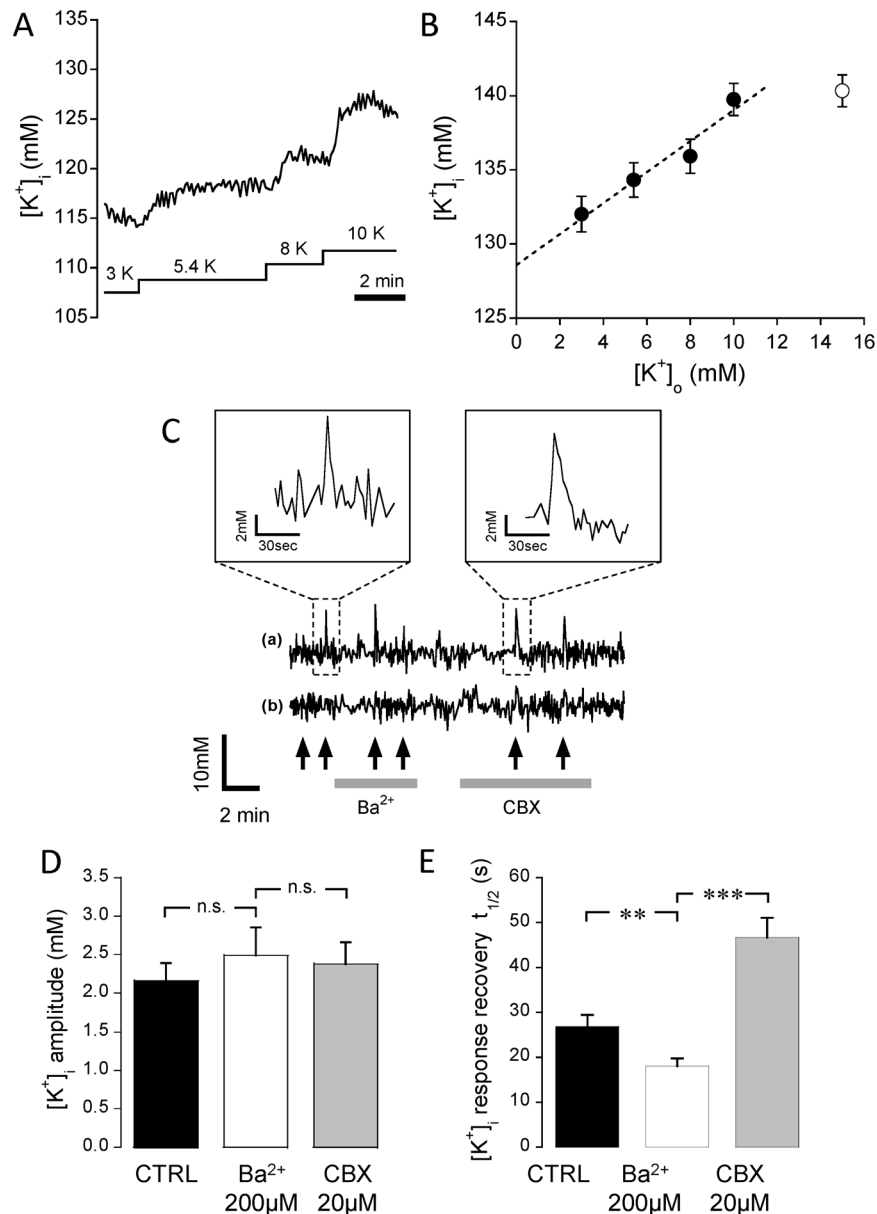


**Figure 3. Intracellular  $K^+$  is modulated by  $[K^+]_o$  level changes.** (A) Representative single-cell  $[K^+]_i$  trace during bath application of solutions with different  $K^+$  concentrations in the range 3 to 10 mM, as are found during physiological and pathological conditions. (B) Relationship between steady-state  $[K^+]_i$  (measured on plateau levels) and externally applied  $[K^+]_o$  ( $n = 120$  cells from 12 exp). The graph indicates a steady increase in  $[K^+]_i$  in the  $[K^+]_o$  range 3–10 mM (plain circles), which yielded a slope of  $1.04 \pm 0.06$  ( $r = 0.82$ ). A higher  $[K^+]_o$  of 15 mM (open circle) failed to further increase  $[K^+]_i$ . (C) Intracellular  $K^+$  is influenced by localized  $K^+$ -gluconate puff applications. Representative  $[K^+]_i$  traces (average values of 7 cells each) during puff application (black arrows) of  $K^+$  gluconate in close proximity to the pipette (upper trace) and at  $>90 \mu\text{m}$  distance (lower trace). Insets: magnification of the trace after single extracellular applications of  $K^+$ . Average amplitude (D) and duration of  $[K^+]_i$  rise (E) induced by  $K^+$  puffs (black bar) compared with responses observed in the presence of 200  $\mu\text{M}$   $\text{Ba}^{2+}$  (white bar) or 20  $\mu\text{M}$  carbenoxolone (CBX, grey bar) ( $n = 62$  cells, 5 exp). No significant changes in amplitudes were found, whereas the response duration was significantly prolonged by CBX and reduced by  $\text{Ba}^{2+}$ . doi:10.1371/journal.pone.0109243.g003

bathochromic shift is frequently observed with fluorescent dyes, including fluorescein, when studied inside living cells, and reflects interactions with intracellular macromolecules [36].

Using this approach, we could measure detectable  $[K^+]_i$  changes in register with bath  $K^+$  concentration changes in the range 3–10 mM  $[K^+]_o$ . This result is in line with previous measurements of  $[K^+]_i$  performed using  $K^+$ -sensitive microelectrodes (see e.g. [12,16]). The fact that no further increase in  $[K^+]_i$  was observed at 15 mM  $[K^+]_o$  is indicative of the presence of a

saturable pathway for  $K^+$  entry and/or a regulatory mechanism. In order to determine whether APG-1 could be used to investigate  $[K^+]_i$  responses to local transient increases in  $[K^+]_o$ , we applied puffs of  $K^+$  from a pipette positioned close to target cells in the field of view. Indeed, such local puffs induced a short-lived but detectable intracellular response consisting in an initial sharp  $[K^+]_i$  rise followed by a slower recovery to baseline. Cells at a distance of  $>90 \mu\text{m}$  from the pipette tip did not exhibit a change in  $[K^+]_i$ . In these experiments, application of  $\text{Ba}^{2+}$  did not inhibit the fast  $[K^+]_i$

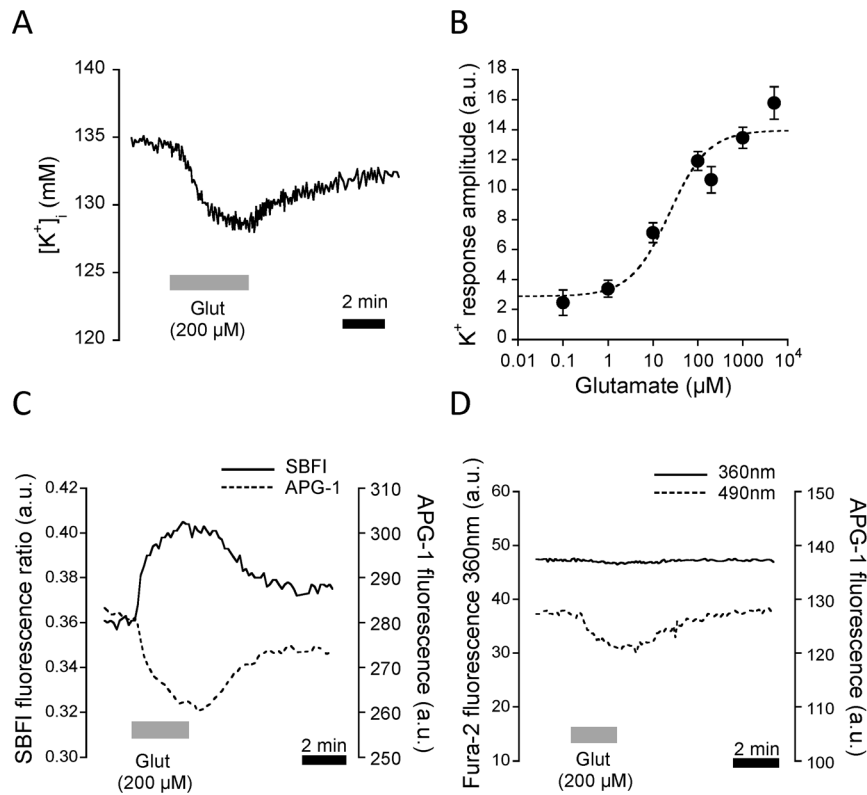


**Figure 4. Intracellular  $K^+$  is modulated by glutamate application.** (A) Application of 200  $\mu$ M glutamate induced a rapid and reversible  $[K^+]_i$  decrease with an amplitude of  $2.3 \pm 0.1$  mM (B) The  $[K^+]_i$  response to glutamate application in the range 0.1  $\mu$ M to 10 mM followed a Michaelis and Menten kinetics with an apparent  $EC_{50}$  of  $11.1 \pm 1.4$   $\mu$ M. (C) Simultaneous  $Na^+$  and  $K^+$  monitoring using SBFI and APG-1, respectively. SBFI was sequentially excited at 340 and 380 nm, and its fluorescence excitation ratio computed, and APG-1 was excited at 490 nm. Glutamate application (200  $\mu$ M) is indicated in the graph. Exemplar single cell trace out of three experiments. (D) The fluorescent dye Fura-2 co-loaded with APG-1 was excited at 360 nm, its  $Ca^{2+}$ -insensitive wavelength, whereas APG-1 was excited at 490 nm. Whereas 200  $\mu$ M glutamate application caused a decline of the APG-1 fluorescence response, that of Fura-2 at 360 nm remained unperturbed (Exemplar trace out of two experiments). doi:10.1371/journal.pone.0109243.g004

response, indicating that  $K_{ir}$  channels were not likely to be directly involved. The exact role and involvement of  $K_{ir}$  channels in  $K^+$  buffering remains a matter of debate [6,37,38] and the repertoire of  $K^+$  conductances underlying the passive conductance of  $K^+$  in astrocytes remains uncertain [4,39]. The fact that  $Ba^{2+}$  did not abolish the  $[K^+]_i$  response, likely indicates that other mechanisms, possibly Na/K/2Cl co-transporters (NKCC1) or the  $Na^+/K^+$  ATPase, are involved, as previously proposed [6]. Members of the two-pore domain  $K^+$  channel family, namely TWIK-1 and TREK-1, have been recently shown to be expressed and functional in astrocytes [39]. Since these channels are resistant to  $Ba^{2+}$ , they could represent an alternative candidate mediating the observed response. In these experiments, the contribution of the astrocytic syncytium in quickly dispersing the increased  $[K^+]_i$  was demonstrated by blocking the gap junctions, which markedly increased the duration of the  $[K^+]_i$  elevation in the stimulated cell.

Here we also demonstrate for the first time, to the best of our knowledge, that  $[K^+]_i$  levels in astrocytes are decreased by the application of glutamate. The observed  $[K^+]_i$  drop is attributable to the activity of glutamate transporters whose transport cycle involves the exchange of one  $K^+$  ion transported out of the cell, with three  $Na^+$  ions and a proton that are co-transported with glutamate into the cell [9,11]. It should be pointed out that the contribution of ionotropic glutamate receptors in the response is unlikely since the application of NMDA does not evoke responses in the primary astrocyte model used in this study [28]. We also

previously showed that AMPA receptor desensitization in primary astrocytes prevents a sizable cation influx that influences intracellular concentrations [23]. The kinetics of the observed response, the simultaneously measured  $Na^+$  rise, and the apparent  $EC_{50}$  of the response to glutamate of 11  $\mu$ M are all identical to that published earlier in similar experimental conditions when measuring the glutamate transport associated  $Na^+$  response in astrocytes [23]. It is worth noting that resting extracellular glutamate is maintained in the low micromolar range. During neuronal activity it has been estimated that glutamate reaches the astrocyte membrane with a concentration that ranges from 10  $\mu$ M [40] to 160–190  $\mu$ M [41]. Our results obtained using primary astrocytes indicate that APG-1 is sensitive enough to detect  $K^+$  changes occurring within the physiological concentration range of glutamate. Whether this is also the case in brain slice astrocytes requires further experimental validation. Given that there should be a ratio of 3:1 of  $Na^+$  versus  $K^+$  movement during each transport cycle, one could postulate that the  $K^+$  response should be three-fold lower than the  $Na^+$  response. However, we observed an amplitude of  $[K^+]_i$  response to glutamate of only 2.3 mM, i.e. about 5–10-fold lower than that of  $[Na^+]_i$  under similar experimental conditions [see e.g. 23]. Therefore, it appears that a concurrent  $K^+$  influx during glutamate application may be rapidly activated to compensate for the cytosolic  $K^+$  drop. One candidate could be the  $Na^+/K^+$  ATPase which undergoes rapid activation during glutamate uptake in astrocytes [23]. While the

$\text{Na}^+/\text{K}^+$  ATPase pumps two  $\text{K}^+$  ions into the cell for 3  $\text{Na}^+$  that are extruded, glutamate transport exchanges one  $\text{K}^+$  for three  $\text{Na}^+$ . Thus, if one considers the  $\text{Na}^+/\text{K}^+$  ATPase and glutamate transport as a functionally coupled complex, as has been suggested [42–44], during glutamate transport, overall the  $\text{K}^+$  influx would be larger than its efflux, possibly explaining the smaller than expected decrease in  $[\text{K}^+]_i$  during glutamate transport. Another alternative could be a possible involvement of mitochondria that have been proposed to sequester  $\text{K}^+$  in astrocytes [21]. Mitochondria have been shown to be actively involved during astrocytic responses to glutamate, in particular by taking up  $\text{Na}^+$  [45] and protons [28] into their matrix. It is conceivable that under these conditions mitochondria, through their ability to take up and release  $\text{K}^+$  may act as intracellular  $\text{K}^+$  buffers and thus reduce the  $[\text{K}^+]_i$  changes. This idea could explain both the  $\text{K}^+$  drop during glutamate transport and the slope of  $[\text{K}^+]_i$  change upon external  $\text{K}^+$  level changes, that were found to be lower than anticipated in the present study.

In conclusion, this study demonstrates that the novel fluorescent  $\text{K}^+$  indicator APG-1 is a powerful new tool that can be employed to address detailed and fundamental questions about the regulation of  $[\text{K}^+]_i$ . Of particular relevance is our novel finding that glutamate uptake by astrocytes has a significant influence on  $[\text{K}^+]_i$ , a finding that represents an important contribution to an integrated understanding of astrocyte functions in the brain.

## References

- Anderson CM, Swanson RA (2000) Astrocyte glutamate transport: Review of properties, regulation, and physiological functions. *Glia* 32: 1–14.
- Kofuji P, Newman EA (2004) Potassium buffering in the central nervous system. *Neuroscience* 129: 1045–1056.
- Amedee T, Robert A, Coles JA (1997) Potassium homeostasis and glial energy metabolism. *Glia* 21: 46–55.
- Olsen M (2012) Examining potassium channel function in astrocytes. *Methods Mol Biol* 814: 265–281.
- Amzica F (2002) In vivo electrophysiological evidences for cortical neuron-glia interactions during slow (<1 Hz) and paroxysmal sleep oscillations. *J Physiol Paris* 96: 209–219.
- Larsen BR, Assentoft M, Cotrina ML, Hua SZ, Nedergaard M, et al. (2014) Contributions of the  $\text{Na}^+/\text{K}^+$ -ATPase, NKCC1, and Kir4.1 to hippocampal  $\text{K}^+$  clearance and volume responses. *Glia* 62: 608–622.
- Langer J, Rose CR (2009) Synaptically induced sodium signals in hippocampal astrocytes in situ. *J Physiol* 587: 5859–5877.
- Pellerin L, Bouzier-Sore AK, Aubert A, Serres S, Merle M, et al. (2007) Activity-dependent regulation of energy metabolism by astrocytes: An update. *Glia* 55: 1251–1262.
- Levy LM, Warr O, Attwell D (1998) Stoichiometry of the glial glutamate transporter GLT-1 expressed inducibly in a Chinese hamster ovary cell line selected for low endogenous  $\text{Na}^+$ -dependent glutamate uptake. *Journal of Neuroscience* 18: 9620–9628.
- Danbolt NC (2001) Glutamate uptake. *Progresses in Neurobiology* 65: 1–105.
- Zerangue N, Kavanaugh MP (1996) Flux coupling in a neuronal glutamate transporter. *Nature* 383: 634–637.
- Ballanyi K, Graf P, ten Bruggencate G (1987) Ion activities and potassium uptake mechanisms of glial cells in guinea-pig olfactory cortex slices. *J Physiol* 382: 159–174.
- Coles JA, Schneider-Picard G (1989) Increase in glial intracellular  $\text{K}^+$  in drone retina caused by photostimulation but not mediated by an increase in extracellular  $\text{K}^+$ . *Glia* 2: 213–222.
- Kettenmann H, Sonnhof U, Schachner M (1983) Exclusive potassium dependence of the membrane potential in cultured mouse oligodendrocytes. *J Neurosci* 3: 500–505.
- Wuttke WA (1990) Mechanism of potassium uptake in neuropile glial cells in the central nervous system of the leech. *J Neurophysiol* 63: 1089–1097.
- Coles JA, Orkand RK (1983) Modification of potassium movement through the retina of the drone (*Apis mellifera* male) by glial uptake. *J Physiol* 340: 157–174.
- Dufour S, Dufour P, Chever O, Vallee R, Amzica F (2011) In vivo simultaneous intra- and extracellular potassium recordings using a micro-optrode. *J Neurosci Methods* 194: 206–217.
- Heinemann U, Lux HD (1975) Undershoots following stimulus-induced rises of extracellular potassium concentration in cerebral cortex of cat. *Brain Res* 93: 63–76.
- Minta A, Tsien RY (1989) Fluorescent indicators for cytosolic sodium. *Journal of Biological Chemistry* 264: 19449–19457.
- Kasner SE, Ganz MB (1992) Regulation of intracellular potassium in mesangial cells: a fluorescence analysis using the dye, PBFI. *American Journal of Physiology* 262: F462–F467.
- Kozoriz MG, Church J, Ozog MA, Naus CC, Krebs C (2010) Temporary sequestration of potassium by mitochondria in astrocytes. *J Biol Chem*.
- Sorg O, Magistretti PJ (1992) Vasoactive intestinal peptide and noradrenaline exert long-term control on glycogen levels in astrocytes: blockade by protein synthesis inhibition. *Journal of Neuroscience* 12: 4923–4931.
- Chatton J-Y, Marquet P, Magistretti PJ (2000) A quantitative analysis of L-glutamate-regulated  $\text{Na}^+$  dynamics in mouse cortical astrocytes: implications for cellular bioenergetics. *European Journal of Neuroscience* 12: 3843–3853.
- Houngaard J, Nicholson C (1983) Potassium accumulation around individual purkinje cells in cerebellar slices from the guinea-pig. *J Physiol* 340: 359–388.
- Pellerin L, Magistretti PJ (1994) Glutamate uptake into astrocytes stimulates aerobic glycolysis: a mechanism coupling neuronal activity to glucose utilization. *Proceedings of the National Academy of Sciences of the USA* 91: 10625–10629.
- Lamy CM, Chatton JY (2011) Optical probing of sodium dynamics in neurons and astrocytes. *NeuroImage* 58: 572–578.
- Kiedrowski L (1999) N-methyl-D-aspartate excitotoxicity: relationships among plasma membrane potential,  $\text{Na}^+/\text{Ca}^{2+}$  exchange, mitochondrial  $\text{Ca}^{2+}$  overload, and cytoplasmic concentrations of  $\text{Ca}^{2+}$ ,  $\text{H}^+$ , and  $\text{K}^+$ . *Mol Pharmacol* 56: 619–632.
- Azarias G, Perreten H, Lengacher S, Poburko D, Demaurex N, et al. (2011) Glutamate transport decreases mitochondrial pH and modulates oxidative metabolism in astrocytes. *Journal of Neuroscience* 31: 3550–3559.
- Bernardinelli Y, Magistretti PJ, Chatton J-Y (2004) Astrocytes generate  $\text{Na}^+$ -mediated metabolic waves. *Proceedings of the National Academy of Sciences of the USA* 101: 14937–14942.
- Rose CR, Karus C (2013) Two sides of the same coin: Sodium homeostasis and signaling in astrocytes under physiological and pathophysiological conditions. *Glia*.
- Leis JA, Bekar LK, Walz W (2005) Potassium homeostasis in the ischemic brain. *Glia* 50: 407–416.
- Walz W (2000) Role of astrocytes in the clearance of excess extracellular potassium. *Neurochem Int* 36: 291–300.
- Somjen GG (2002) Ion regulation in the brain: implications for pathophysiology. *Neuroscientist* 8: 254–267.
- Langer J, Stephan J, Theis M, Rose CR (2012) Gap junctions mediate intercellular spread of sodium between hippocampal astrocytes in situ. *Glia* 60: 239–252.
- Gardner-Medwin AR, Nicholson C (1983) Changes of extracellular potassium activity induced by electric current through brain tissue in the rat. *J Physiol* 335: 375–392.
- Meisinger KK, Steen HB (1981) Intracellular binding of fluorescein in lymphocytes. *Cytometry* 1: 272–278.
- Hertz L, Xu J, Song D, Yan E, Gu L, et al. (2013) Astrocytic and neuronal accumulation of elevated extracellular  $\text{K}^+$  with a 2/3  $\text{K}^+/\text{Na}^+$  flux

## Supporting Information

**Figure S1 Spectrofluorimetric characterization of the influence of  $\text{Na}^+$  on APG-1 fluorescence.** Fluorescence emission plotted as a function of  $\text{Na}^+$  concentration in intracellular-like solution containing increasing concentrations of  $\text{K}^+$  (0–150 mM). The total monovalent cation concentration was kept constant by appropriate additions of NMDG. Each curve represents triplicate measurements. (TIF)

## Acknowledgments

We thank Dr. Akwasi Minta (Teflabs) for continuous fruitful interactions and advice regarding fluorescent probes, Enea Pianezzi for his help with the spectrofluorimetric analysis, and Jennifer Luebke (Boston University) for her critical reading of the manuscript.

## Author Contributions

Conceived and designed the experiments: TSR JYC. Performed the experiments: TSR JYC. Analyzed the data: TSR JYC. Contributed to the writing of the manuscript: TSR JYC.

- ratio-consequences for energy metabolism, osmolarity and higher brain function. *Front Comput Neurosci* 7: 114.
38. D'Ambrosio R, Gordon DS, Winn HR (2002) Differential role of KIR channel and Na<sup>+</sup>/K<sup>+</sup>-pump in the regulation of extracellular K<sup>+</sup> in rat hippocampus. *J Neurophysiol* 87: 87–102.
  39. Zhou M, Xu G, Xie M, Zhang X, Schools GP, et al. (2009) TWIK-1 and TREK-1 are potassium channels contributing significantly to astrocyte passive conductance in rat hippocampal slices. *J Neurosci* 29: 8551–8564.
  40. Lalo U, Pankratov Y, Kirchhoff F, North RA, Verkhratsky A (2006) NMDA receptors mediate neuron-to-glia signaling in mouse cortical astrocytes. *J Neurosci* 26: 2673–2683.
  41. Dzubay JA, Jahr CE (1999) The concentration of synaptically released glutamate outside of the climbing fiber-Purkinje cell synaptic cleft. *Journal of Neuroscience* 19: 5265–5274.
  42. Cholet N, Pellerin L, Magistretti PJ, Hamel E (2002) Similar perisynaptic glial localization for the Na<sup>+</sup>,K<sup>+</sup>-ATPase alpha 2 subunit and the glutamate transporters GLAST and GLT-1 in the rat somatosensory cortex. *Cereb Cortex* 12: 515–525.
  43. Matos M, Augusto E, Agostinho P, Cunha RA, Chen JF (2013) Antagonistic Interaction between Adenosine A2A Receptors and Na<sup>+</sup>/K<sup>+</sup>-ATPase-alpha2 Controlling Glutamate Uptake in Astrocytes. *J Neurosci* 33: 18492–18502.
  44. Rose EM, Koo JC, Antflick JE, Ahmed SM, Angers S, et al. (2009) Glutamate transporter coupling to Na<sup>+</sup>,K<sup>+</sup>-ATPase. *J Neurosci* 29: 8143–8155.
  45. Bernardinelli Y, Azarias G, Chatton J-Y (2006) In situ fluorescence imaging of glutamate-evoked mitochondrial Na<sup>+</sup> responses in astrocytes. *Glia* 54: 460–470.